Continuous hourly bio-optical observations of chlorophyll fluorescence and turbidity off Cape Ann, Massachusetts reveal large interannual variations in phytoplankton blooms and turbidity

Massachusetts Water Resources Authority
Environmental Quality Department
Report 2026-08

Citation:

Roesler, Collin. 2026. Continuous hourly bio-optical observations of chlorophyll fluorescence and turbidity off Cape Ann, Massachusetts reveal large interannual variations in phytoplankton blooms and turbidity. Massachusetts Water Resources Authority. Report 2026-8. 20 p.

Continuous hourly bio-optical observations of chlorophyll fluorescence and turbidity off Cape Ann, Massachusetts reveal large interannual variations in phytoplankton blooms and turbidity.

Principal Investigator:	Dr. Collin Roesler
Institution:	Bowdoin College Department of Earth and Oceanographic Science
Address:	6800 College Station Brunswick, ME 04011
Phone:	207-725-3842
Email:	croesler@bowdoin.edu

Period of Performance:	1 July 2025 - 30 June 2026

HIGHLIGHTS

The setting: For 25 years, the Massachusetts Water Resources Authority (MWRA) has discharged treated wastewater from its Deer Island Treatment Plant in Boston through a 15 km (9 mi) tunnel into Massachusetts Bay. MWRA has supported a monitoring program to determine whether the nutrient discharge contributes to excess phytoplankton growth.

Moored observations: Starting in July 2001, a real-time reporting buoy measuring ocean physical properties (e.g., temperature, salinity and currents) was deployed in northeastern Massachusetts Bay off Cape Ann by the University of Maine (www.gyre.umeoce.maine.edu), supported by the Northeast Regional Association of Coastal Ocean Observing Systems (www.neracoos.org) and MWRA. Bio-optical sensors were added to the mooring in 2005 by Bowdoin College researchers with support from MWRA. These sensors provide hourly observations of near surface chlorophyll fluorescence (a proxy for phytoplankton concentration) and turbidity (a proxy for suspended particle concentration).

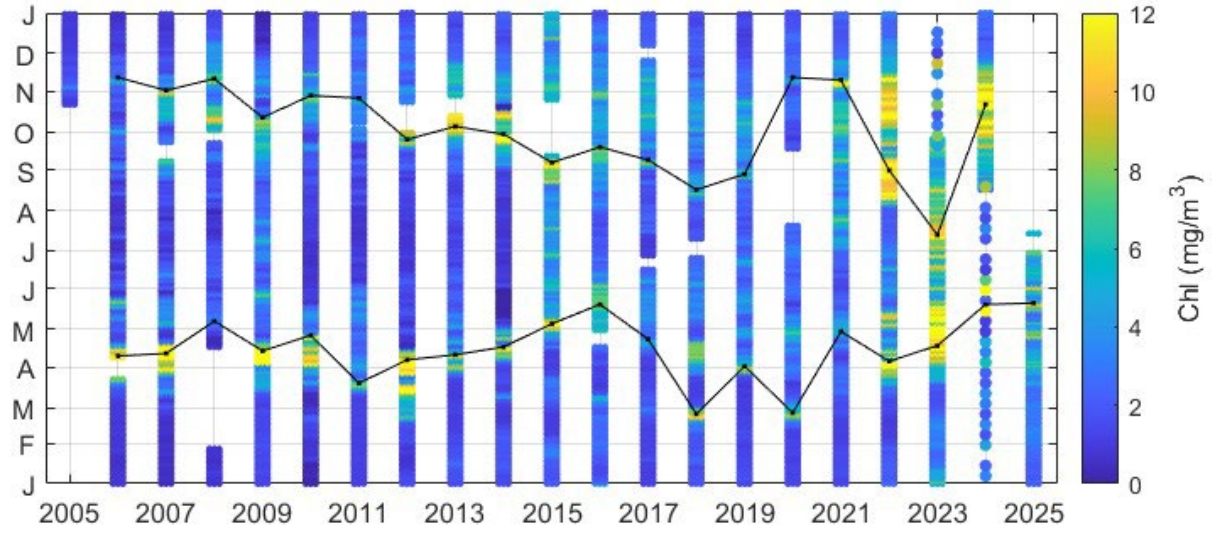

Seasonal patterns of daily chlorophyll concentration from A01 since 2005. Date of maximal concentrations Jan-June and July-Dec representing spring and fall blooms, respectively, indicated by black lines. Missing data from deployment A0147 (Oct 2023-August 2024, circle symbols) are augmented with satellite estimates (Roesler 2025).

Results from the 2024-25 deployment: Continuous hourly bio-optical observations for deployment A0149 covered the interval between 15 December 2024 and 14 June 2025, followed by patchy observations until June 29th, and a data gap until the final date of the deployment on July 31, 2025. The seasonal pattern in the phytoplankton community at the Cape Ann mooring is characterized by spring and fall blooms, the timing, intensity and duration of which vary from year to year. The emergence of multiple high intensity blooms from April to November for the years 2022-2024 appears to have weakened in 2025, although late spring to summer concentrations are elevated compared to years prior to 2015. Turbidity values for deployment A0149 are also lower than in recent years, with values comparable to the years of lowest magnitude.

INTRODUCTION

This report describes work and results for MWRA's continuous biological monitoring in Massachusetts Bay performed by Bowdoin College researchers for all deployments recovered within the contract period 1 July 2025 through 30 June 2026 (i.e., deployment 49). While the focus of the report is on the observations from the current reporting year, the overall program goal is to establish benchmark values for seasonal variations in the concentrations of phytoplankton and suspended particles to contextualize the current year observations. This report provides MWRA with the ability to identify and respond to critical changes in phytoplankton concentration. The permit to discharge treated effluent from the Deer Island Wastewater Treatment Plant into Massachusetts Bay requires the specific monitoring elements that are outlined in MWRA's Ambient Monitoring Plan. The moored bio-optical program is an important element in the Plan (Figure 1). The details of the moored bio-optical observations are provided in prior annual reports (e.g., Roesler 2016, 2020, 2021). Important elements of the bio-optical monitoring are summarized below.

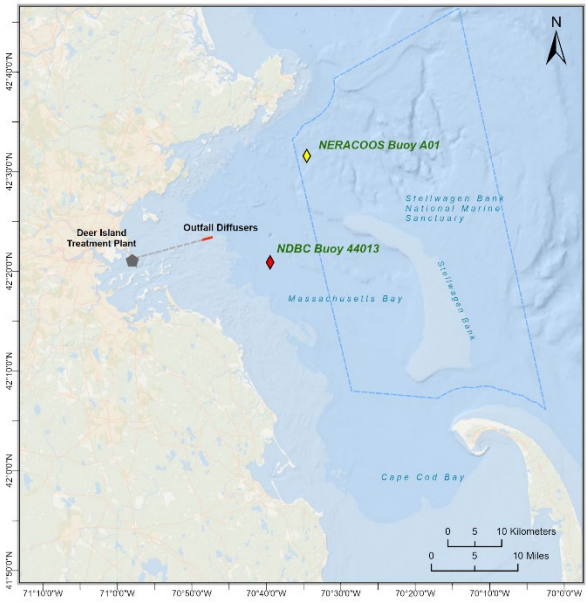

Figure 1. Bathymetric map of Massachusetts Bay showing the location of the Deer Island Treatment Plant, outfall diffusers, NERACOOS Buoy A, and NDBC Buoy 44013.

The bio-optical data set consists of **three types of measurements**: chlorophyll fluorescence, turbidity, and solar irradiance. Each measurement is described below.

Chlorophyll *a* (Chl) is a photosynthetic pigment found in all marine phytoplankton. No other planktonic organisms synthesizes it and thus provides a unique proxy for phytoplankton concentration. The molecule absorbs light in both the blue and red wavebands (Figure 2). Phytoplankton in the natural environment have additional accessory pigments that fill in absorption gap in the blue-green wavelength range. In combination with water absorption, which increases from yellow to red, the solar radiation that emanates from the ocean's surface transitions from blue to green as the concentration of phytoplankton increases. Thus, phytoplankton blooms are largely responsible for the "greening" of the ocean that is visible by eye and detected by satellite sensors. A unique characteristic of the Chl molecule is that a portion of the energy it absorbs directly, or energy that is transferred to it from the accessory

pigments, is emitted (fluoresced) as red light (Figure 2). Fluorometers target phytoplankton absorption in the blue to blue-green range using excitation with narrow waveband LEDs and detect the resulting Chl fluorescence in the red, effectively avoiding other seawater constituents.

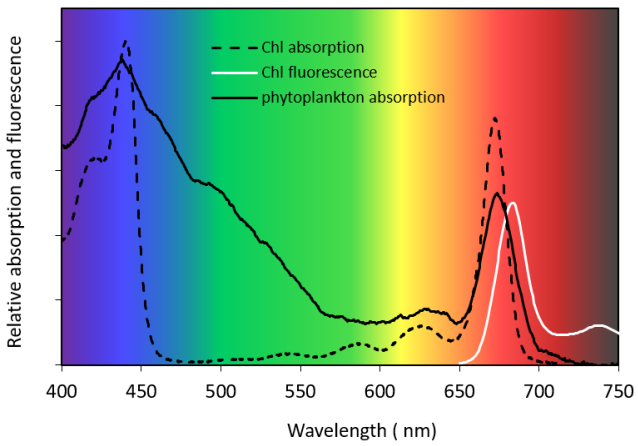

Figure 2. Absorption spectra for the chlorophyll *a* molecule (dashed line) and an average phytoplankton population (solid line), and fluorescence spectrum for the chlorophyll *a* molecule (white line), over the visible spectrum from blue to red. Chl absorbs in the blue and red wavebands and fluoresces at longer red wavelengths. Phytoplankton have additional accessory pigments that absorb in the blue to green wavebands and pass the energy to Chl, stimulating fluorescence in living cells.

Turbidity is general term defined as water cloudiness due to suspended microscopic particles such as sediments, phytoplankton, and bacteria. The cloudiness, or lack of clarity, is caused by the scattering of light by suspended particles. Numerous optical sensors output values of "turbidity" by measuring some portion of scattered light. Scattering in the backward direction is least sensitive to variations in particle size; scattering in the red wavebands is least sensitive to variations in particle composition (because particle absorption is minimal in the red for all constituents). Thus, quantitative turbidity sensors measure particle scattering in the red wavelengths over a broad angle range in the backscattering direction to provide a robust proxy for particle concentration.

Solar irradiance is a measure of the intensity of sunlight in the visible waveband incident on the sea surface. A portion of the incident irradiance penetrates the upper ocean, resulting in the lit euphotic zone. Phytoplankton in the lit zone absorb solar radiation proportional to their pigment absorption spectra (Figure 2); the absorbed energy drives photosynthesis. Strong intensities of solar radiation can inhibit both photosynthesis and fluorescence, a process called non-photochemical quenching. It is important to quantify the amount of quenching to correct measurements of Chl fluorescence and avoid underestimating Chl concentration. Solar irradiance is also the driving factor for warming the surface layer of the ocean (called shortwave warming), decreasing its density, and increasing thermal stratification.

Three sensor models are used to collect the bio-optical measurements: two are located 3 m below the sea surface, and one is mounted atop the buoy infrastructure. The in-water package consists of an FLNTU, a combination Chl fluorometer and turbidity sensor, and an F3WB, a Chl fluorometer with three excitation LEDs that stimulate Chl fluorescence at three different wavelengths. The solar irradiance sensor (OCA507) is deployed at the top of the buoy infrastructure about 3 m above the surface. All 3 sensors are controlled by a data and power

handler (DH4) that brings power from the buoy solar panels to the sensors and relays hourly values back to the buoy data controller (Campbell data logger) for near-real-time telemetry.

The two sensors that measure **Chl fluorescence** consist of light emitting diodes (LEDs) that emit a flash of light in a narrow wavelength band within the blue to green region of the spectrum where phytoplankton pigments absorb energy for photosynthesis (Figure 2). The sensors measure the intensity of the red light fluoresced by Chl in phytoplankton cells within a known seawater volume defined by the intersection of the LED light cone and the detection cone (Figure 3A). The FLNTU Chl fluorometer (Figure 3B) utilizes a 470 nm blue LED for excitation of accessory pigments that stimulate Chl fluorescence. It has a rotating shutter to minimize biofouling on the optical face. The FL3WB, first deployed in 2016, was added to the package to (1) provide redundancy of the 470 nm excitation, (2) add two additional LED colors (440 nm and 532 nm) that probe different phytoplankton pigments yielding qualitative information about phytoplankton community composition, and (3) minimize the impacts of biofouling via an automated wiper that reduces biofouling due to flora and faunal growth and biofilms on the optical head (Figure 3C). All of the Chl fluorometers are calibrated at Bowdoin College to provide Chl concentrations that are robust within each deployment and across deployments with different sensors (Roesler et al., 2017).

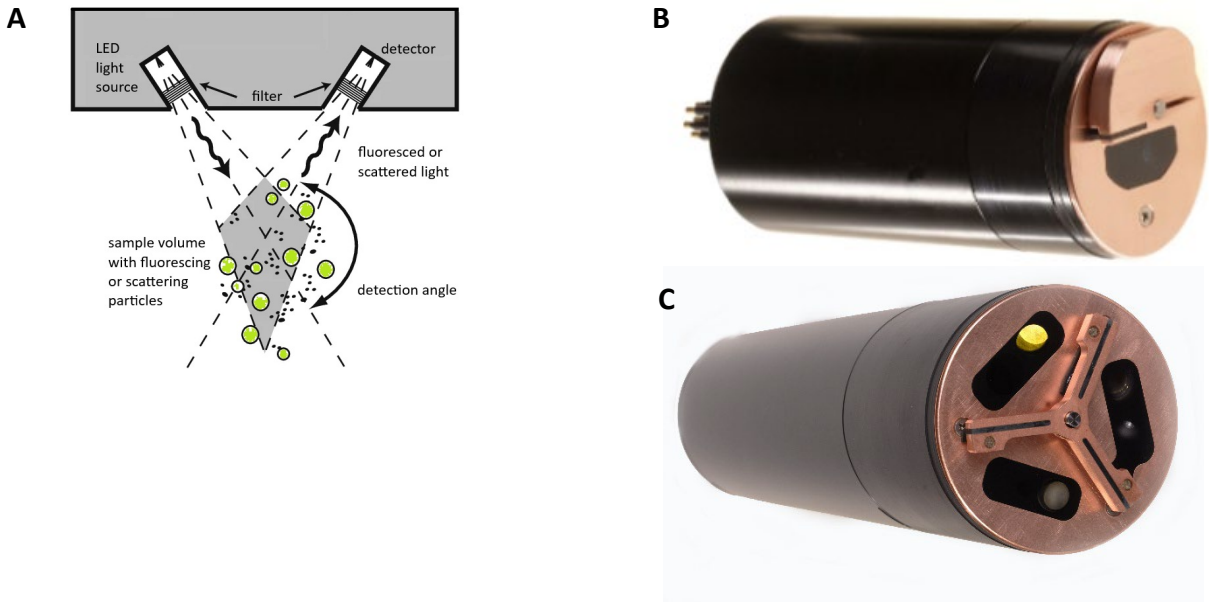

Figure 3. A. Schematic of WETLabs ECO sensors with LED excitation, detection, and shaded seawater sample volume for detected fluorescence and backscattering, B. FLNTU sensor with copper face and shutter, C. side and optical face view of FL3WB showing 3 LED-detector optical pairs, copper face, and automatic wiper.

The FLNTU **turbidity** sensor emits an LED flash of red light (660 nm) and measures the intensity of that red light scattered backward out of a known seawater volume by suspended particulate matter (Figure 3A). The turbidity sensor is calibrated to provide robust, quantitative estimates of suspended particles within each deployment and across deployments with different sensors.

Solar irradiance in seven visible wavebands from blue to red (~410 nm to 680 nm) is measured with an irradiance sensor that sits on top of the mooring. It is used to improve the estimate of chlorophyll concentrations derived from fluorescence measurements as intense sunlight can reduce (quench) the capacity for phytoplankton to fluoresce (Carberry et al. 2019). It can also be used to model primary productivity and to quantify the proportion of sunny and cloudy days if there is interest.

The **focus of this report** is presentation and analysis of the data from deployment A0149, the 49th deployment of the mooring A01, covering the dates 15 December 2024 through 31 July 2025, which was recovered within the 2025-26 contract year. These data have been added to the MWRA data archive, and this report includes brief descriptions of the quality assurance and analysis methods, and bio-optical interpretations of all years of data.

SENSORS AND DATA RECOVERY

Details on the bio-optical sensors and their calibration protocols have been outlined in previous reports (e.g., Roesler 2016) and papers (Proctor and Roesler 2010; Roesler et al. 2017). Two sensors of each type (Table 1) are dedicated to this monitoring program. This redundancy allows for two complete sensor packages at all times; one deployed on the mooring, while the second is prepared for the next deployment, with sufficient time for sensor maintenance and calibration. Sensors are sent to the WETlabs facility of Sea-Bird Scientific for maintenance, repair, and calibration as needed between deployments. For the last few years, the turn-around time has exceeded the interval between deployments. In response, Bowdoin researchers have integrated additional sensors to the rotation as needed. They also perform routine maintenance, repair, and calibration on all sensors between every deployment.

Table 1. Components of the optical sensing package on the buoy. Text in parentheses indicates how the instrument is referred to in this report.

INSTRUMENT	PURPOSE
WETLabs ECO FLNTU ("FLNTU")	Optical sensor, measures chlorophyll fluorescence (470 nm excitation LED, 695 nm detection) and turbidity (660 nm excitation LED, 660 nm detection), located at 3 m depth, equipped with automated shutter.
WETLabs ECO FL3-WB ("F3WB")	Optical sensor, measures chlorophyll fluorescence (3 excitation wavelengths, 440 nm, 470 nm, 532 nm, and 695 nm detection), located at 3 m depth, equipped with an automated anti-biofouling wiper.
Satlantic OC507-ICSA ("OCA507")	Optical sensor, measures solar irradiance at 7 visible wavebands; mounted on the buoy tower.
WETLabs DH4 ("DH4")	Data logger, collects and stores data from optical sensors; computes hourly mean values from FLNTU, F3WB, and OCA507 sensors, which are transmitted hourly to Campbell Scientific Data Logger as part of the real time data stream reported by the University of Maine data portal.

The sequence of bio-optical observations from data collection to analysis is as follows. Each hour, the Campbell Scientific data logger sends power to the DH4 data handler, which starts the sampling protocols for the bio-optical sensors. All three sensors collect a "burst" of approximately 60 samples for one minute (e.g., 1 Hz data collection rate). The FLNTU and F3WB sensors have the capacity to store the first 3 months' worth of observations, where as the OCA507 does not. All sensors send the complete data stream in real time to the DH4, which stores the complete set of burst samples, computes hourly averaged values, and sends those values to the Campbell data logger for telemetry. Data limitations of the Campbell are such that the signal from the F3WB 532 nm channel is not included in the telemetered data stream, but the raw burst data are stored on the DH4 and available upon recovery. The data stream from the FLNTU is parsed, calibrations are applied, and the data are made available in real time at the online data portal http://gyre.umeoce.maine.edu/data/gomoos/buoy/html/A01.html and sent to the NERACOOS portal www.neracoos.org. This approach provides a measure of failsafe redundancy. In the event the communication with the Cambell data logger breaks down, the data set is stored on the DH4. If the DH4 fails, the ECO sensors store 3 months of data.

Once the deployment is recovered, the bio-optical sensors are returned to the Bowdoin researchers' lab. The raw data streams from the complete burst sampling are downloaded from the DH4. Synchronization of the internal clocks on the sensors, the DH4, and the Campbell is verified, and any corrections applied. The median and standard deviation values for each hourly burst sample are computed across the sensors. The result is a time series of robust hourly values of each optical data stream. Description of the sensor data streams, and the information derived from them is detailed in Roesler (2021).

The 7-step post-processing protocol for the real-time data for quality control

As explained in detail in prior reports (e.g., Roesler 2020, 2021, 2022), a series of processing steps are necessary to maintain the high quality of the dataset.

Step 1. Quality assurance on times recorded by the sensors, DH4, and the Cambell data logger. Sensors record UCT time vectors which are converted to local standard time (EST).

Step 2. Calibration comparison between sensors of adjacent deployments; correction as required.

Step 3. Correction for sensor drift from preceding and subsequent deployments.

Step 4. Identification, flagging, and removal of biofouled data.

Step 5. Identification, flagging, and correction of chlorophyll fluorescence observations impacted by non-photochemical quenching (NPQ; Carberry et al. 2019).

Step 6. Removal of single value outliers (SVOs).

Step 7. Identification of values below minimum detection levels (MDLs) and within MDL of zero.

Details and examples for all steps other than #2 can be found in Roesler (2020); details and examples for step #2 can be found in Roesler (2021). A graphical representation of the data flagging steps for each sensor can be found in Roesler (2020).

Data products provided. In order to give a clear sequence of observations, flagging and correction steps, we provide hourly data arrays including each stage of the post-processing. These are also helpful for optimization of correction schemes for biofouling and NPQ.

Separate data files are submitted for:

- the chlorophyll (Chl) and turbidity (NTU) sensors of the FLNTU,
- each channel of the calibrated ECO F3WB chlorophyll fluorometer (F1 through F3),
- the 7-channel irradiance (ED7).

The Appendix provides data string formats:

Table A1 provides the data string for hourly chlorophyll fluorescence data obtained from the FLNTU and F3WB sensors.

Table A2 provides the data string format for the hourly turbidity.

Table A3 provides the data string format for the hourly downwelling irradiance and upwelling radiance data files.

Table A4 provides a list of the data file names, descriptions, units and array sizes.

The data arrays provided have the Matlab binary storage "mat" file format.

RESULTS AND DISCUSSION

Time series bio-optical observations. The time series bio-optical observations from the FLNTU span October 2005 through July 2025 (deployments A0115-A0149) and those from the F3WB and irradiance sensors span from July 2016 to July 2025 (deployments A0137-A0149). Deployment A0149 stopped reporting hourly in mid-June 2025 but continued to report sporadically until the end of June, with no data for the final month of the deployment (July). The irradiance sensor reported solar values prior to deployment and after recovery, but the values recorded during the deployment were consistent with those for a capped sensor.

Measurements from the most recent deployment exhibit lower values and lower variability in both Chl and turbidity than had been observed in the previous 3 years from 2022 through 2024 (Figure 4). The spring bloom in 2025 was significantly lower than the preceding fall bloom of 2024. Similarly, the turbidity was also lower than had been observed in 2023.

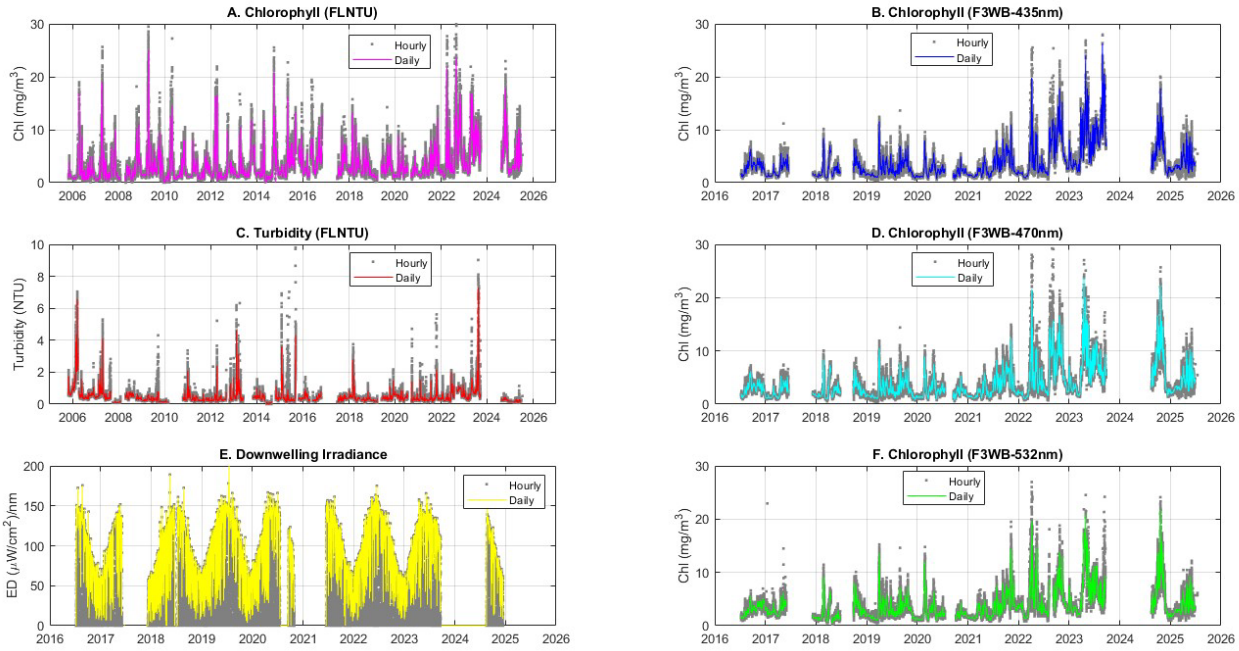

Figure 4. Time series of hourly values (gray symbols) and daily median values (colored lines) from observations of chlorophyll fluorescence (A: FLNTU, 2005-2025; B, D, and E: F3WB, 2016-2025), turbidity (C: FLNTU, 2005-2025), and solar irradiance (E: 2016-2024). Daily maximum values shown for irradiance. Missing data from deployment A0147 in late 2023 through summer 2024 is discussed in Roesler (2025).

Decadal Seasonal Cycles

Seasonal cycles are evident in the monthly climatological median values for all bio-optical observations (Figure 5). Spring and fall blooms are observed in all Chl data streams. Over the first decade of observations (Figure 5A) blooms peaked in April and October with minimum values in January and July. The largest variations were observed during the bloom months in April and July, followed by the months adjacent to blooms, March, May and September. During the last decade (Figure 5B), the spring bloom has increased its duration into May. The magnitude of the fall blooms has increased by about 25% from a median of 4 (mg/m^3) to 5 (mg/m^3) and the duration has increased by one month due to a shift in the onset of the bloom from September to August. Summer and winter minimum values are also increased by up to a factor of 2. This decadal pattern is observed in the F3WB time series for all channels (Figure 5 C, F, H) which was recording data for the same time interval. The most recent deployment (A0149) exhibits values higher than the decadal means January through June, but within the decadal standard deviation (except for the FLNTU in June, which is slightly higher). This is in keeping with recent trends toward higher late spring to early summer (April to June) phytoplankton concentrations compared to the April spring bloom peaks. The monthly variability is also much greater in this second decade.

Turbidity exhibited a slight seasonal pattern in the first decade (Figure 5D) with slightly larger monthly median values and significantly larger monthly standard deviations in the winter and in September. This pattern has been interpreted as the times of weakest stratification (or onset of destratification in September) combined with increased seasonal wind mixing and resuspension of particles from the seafloor. The monthly median values were not significantly different in the most recent decade (Figure 5E), but the wintertime standard deviations were much lower, except for August.

Irradiance is maximal in June and minimal in December consistent with summer and winter solstice (Figure 5G). Variability is higher in the summer and lower in the winter due to the seasonality of clouds.

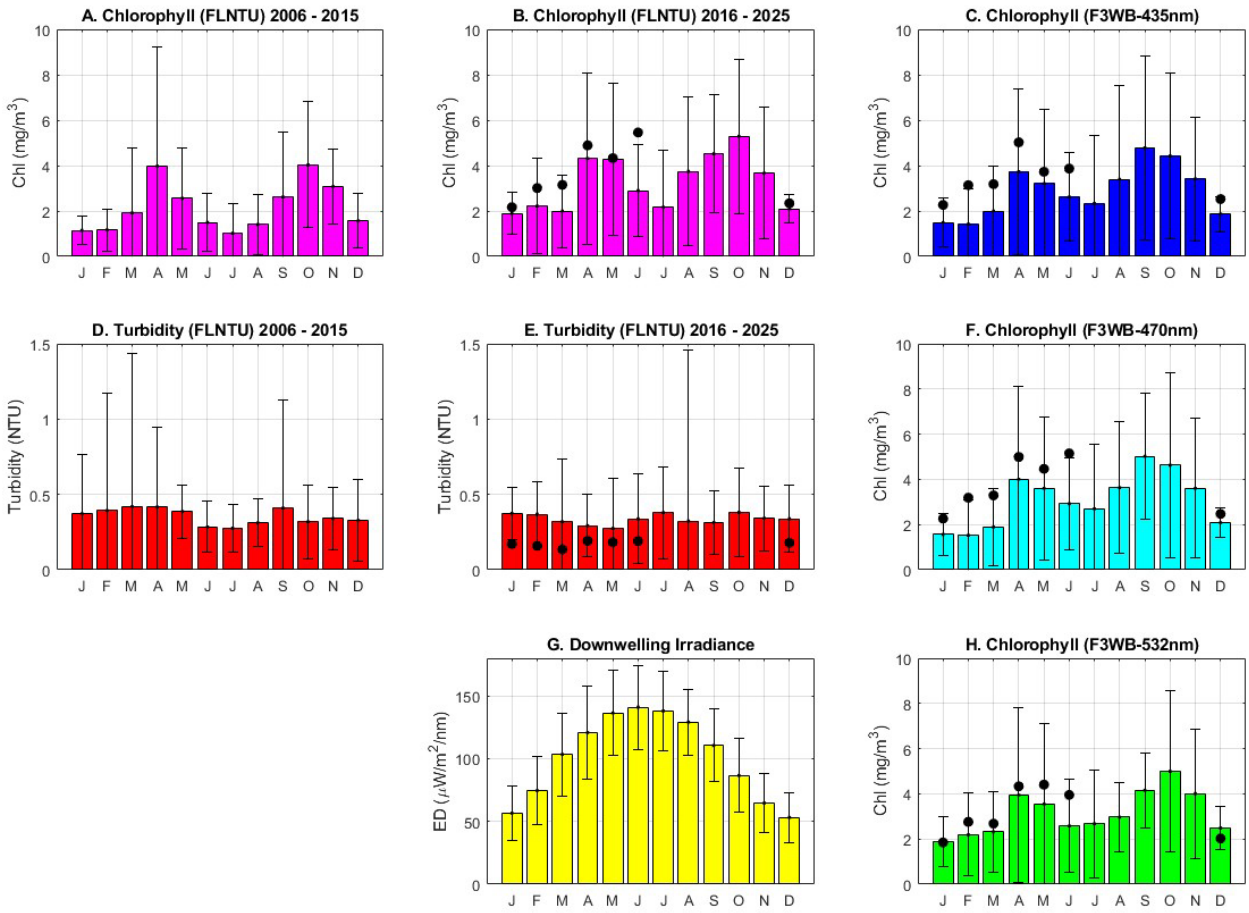

Figure 5. Monthly median values of chlorophyll fluorescence, turbidity and irradiance: (A and B) chlorophyll and (D and E) turbidity from the FLNTU separated by decade; (C, F, and H) F3WB chlorophyll and (G) irradiance since 2016. Bars indicate the median values, and error bars indicate standard deviation. Black symbols are monthly median values for deployment A0149.

Interannual Variability in Phytoplankton Blooms

The change in the timing, intensity and duration of phytoplankton blooms suggests both a long-term trend and increased variability (Figure 6). Spring blooms typically occurred in April from 2006 to 2015, although they increased from early April to mid-May from 2011 to 2016. From 2016 to 2021 the timing of the spring bloom was variable (February to May). The onset of fall blooms became steadily earlier from mid-November to mid-August from 2006 to 2019. A dramatic change in phytoplankton patterns occurred in 2021 when the magnitude of the spring bloom was small and the onset of the fall bloom started in July and peaked in November. The following 3 years exhibited multiple intense blooms spanning April through November. The concentration of phytoplankton in 2025 (A0148 and A0149) was lower than the previous three years but still exhibited highest values in the late spring and summer.

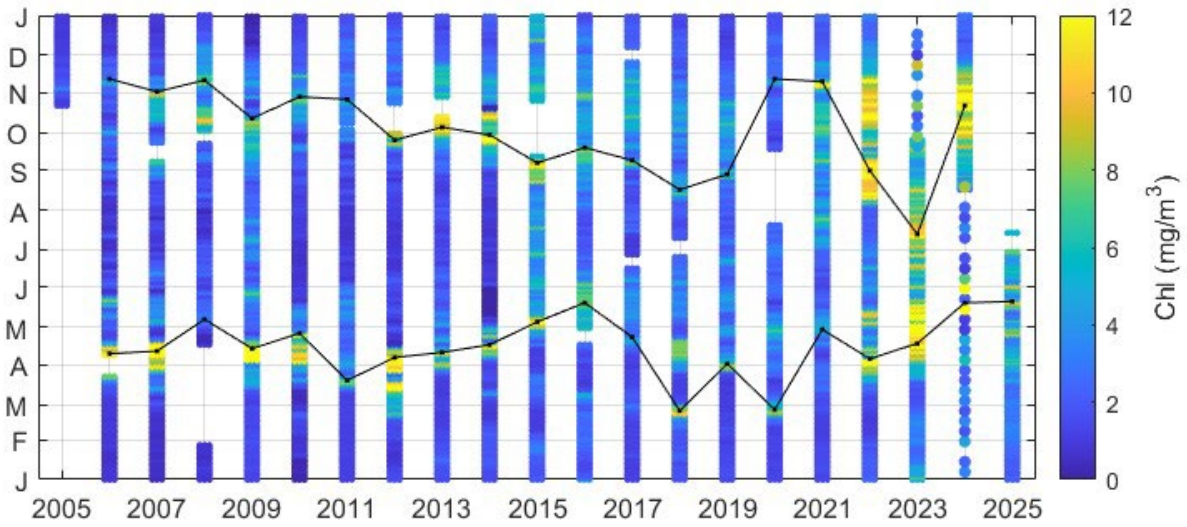

Figure 6. Daily values of (FLNTU) Chl concentration for each month (y-axis) showing seasonality for each year (x-axis) from 2005 to 2026. Gaps in 2023-24 associated with deployment A0147 are interpolated 8-day MODIS observations (see Roesler 2025 for details). Black lines show the peak spring and fall phytoplankton blooms.

Annual Trends

On an annual basis, phytoplankton concentration experienced an increase from 2005 to 2024 (Figure 7) from a median value of approximately 1 mg/m^3 to 6 mg/m^3. The pattern is not monotonic, but displays three peaks of increasing magnitude in 2009, 2015, and 2023. Deployment A0149 (and real-time data from FLNTU A0150) suggest a drop in the annual median by a factor of two. The next year or two will determine if this is a trend or a one-of event. Turbidity (Figure 7C) was highest in 2006 (2005 is not significant as it was a partial year)

and 2023 with a return to lower values starting in 2024. Solar irradiance (Figure 7E) exhibits relatively little year-to-year variations.

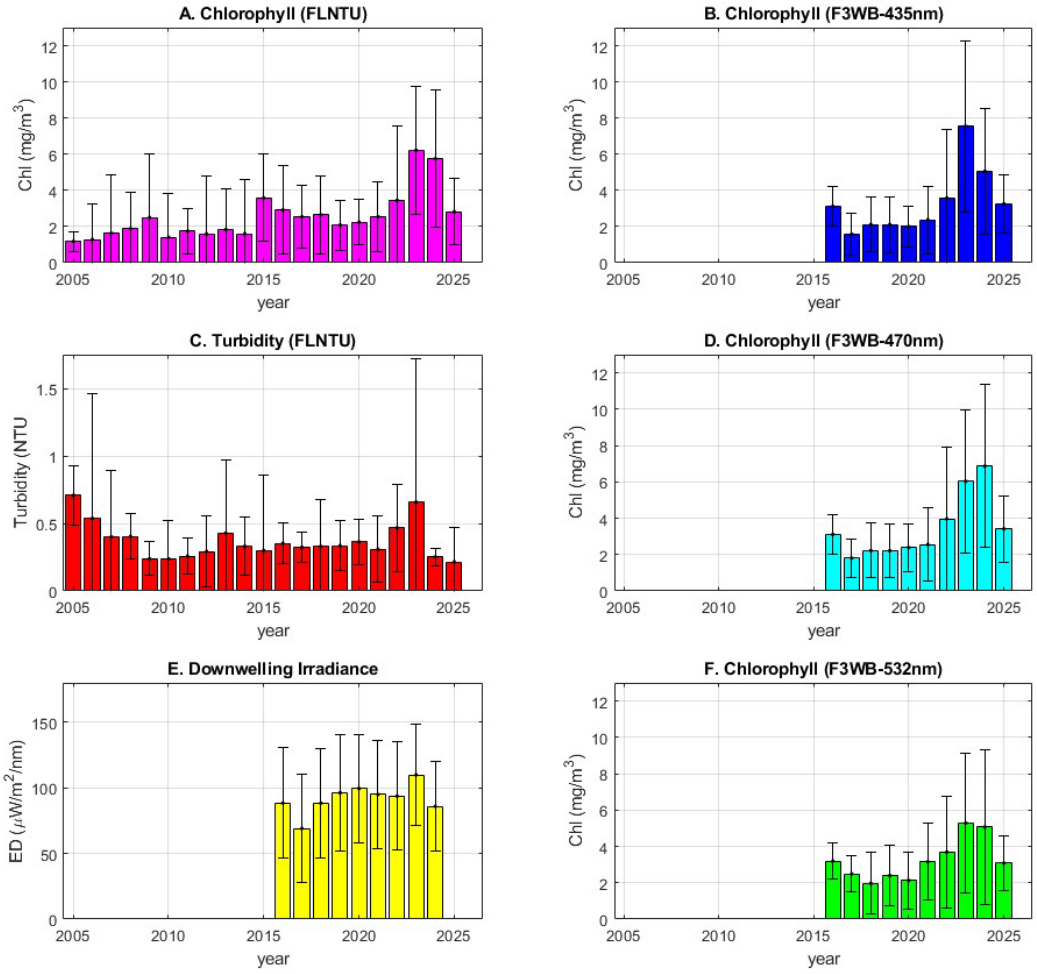

Figure 7 . Annual median values for FLNTU (A) chlorophyll and (C) turbidity, F3WB Chl from (B, D, F) 435 nm, 470 nm, 532 nm excitation, and (E) OCR507A downwelling irradiance. Error bars indicate one standard deviation about the annual median value. Real time Chl and turbidity values from the A0150 observations in 2025 are included in mean and standard deviation to enable accurate comparisons with preceding years.

A single analysis of variance (ANOVA) of the daily Chl observations provides some statistical assessment of the year-to-year changes in concentration. A whisker-plot representation (Figure 8) demonstrates the consistency of the median annual chlorophyll observations from 2005 through 2021. The 25th and 75th percentiles are also generally consistent with the narrowest range observed in 2006 and 2020 and the largest range observed in 2016 until 2022. From 2022 through 2024 there was an increase in both the chlorophyll median value and the range. One of the outcomes of the larger overall variability in those three years is that there are fewer data

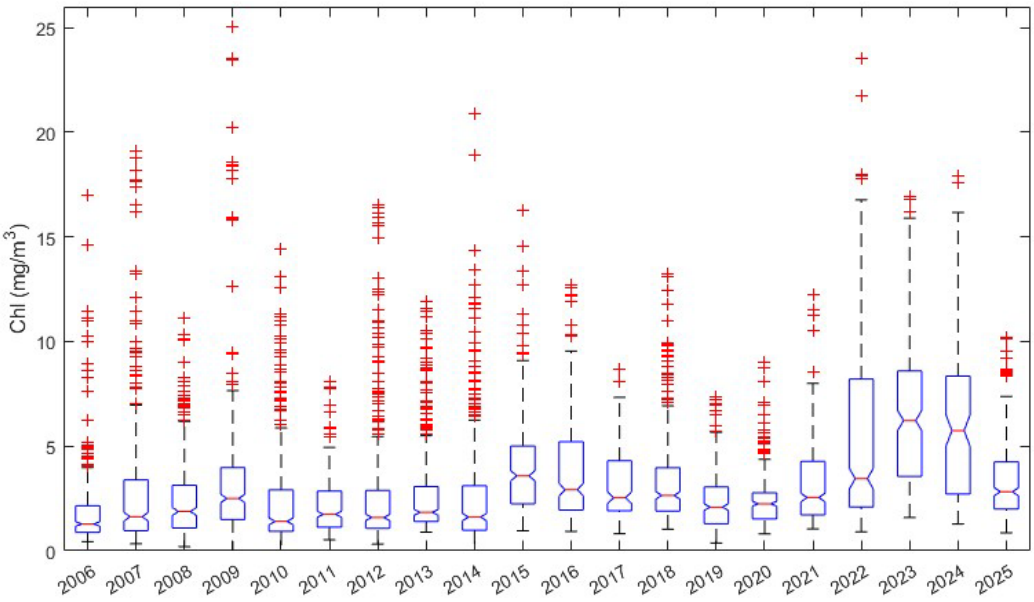

Figure 8. Whisker plot results of the analysis of variance (ANOVA) of daily chlorophyll values from FLNTU chlorophyll observations over the 2005 to 2025 time series with the data gaps from A0137 filled in with MODIS data and July through December 2025 data from A0150. The red bar is the annual median value, the blue box limits show the 25th and 75th percentile range, the error bars indicate the range of all values not identified as outliers and the red + symbols are the outlier values that are 3 standard deviations from the median.

points identified as "outliers" compared to years with overall lower variability. This is consistent with the interpretation that the higher values observed recently are associated with more blooms that have durations on the order of weeks, in contrast to short-lived independent episodic high values observed sporadically in previous years. Deployment A0149 (and the real-time FLNTU values from A0150) exhibit both lower medians, smaller variance and few outliers. A comparison test (Figure 9) of the 2025 annual median value to all other years in the time series show that it is statistically lower than the 2022-2024 years and generally statistically similar to about half of the remaining years throughout the time series, albeit higher than the 20-year median value of 2.27 mg/m^3.

As of the preparation of this report, the hydrographic data for A0149 has not been released and thus an analysis of the pattern and intensity of seasonal stratification cannot be provided to give context to the change in Chl observed in the A0149 deployment relative to the previous 3 years. The increase in annually average Chl values for 2022 through 2024 are primarily driven by the multiple intense summer blooms. These blooms indicate a source of summertime nutrients in the surface waters that is typically kept low due to seasonal stratification and early nutrient drawdown. Reduced stratification coupled with wind mixing events could be the injection mechanism driving summer blooms. Analysis of the 2025 and 2026 hydrologic data will provide some evidence for quantifying the stratification aspect of the story. Deep water nutrient observations would provide evidence for changing source water concentrations fueling blooms.

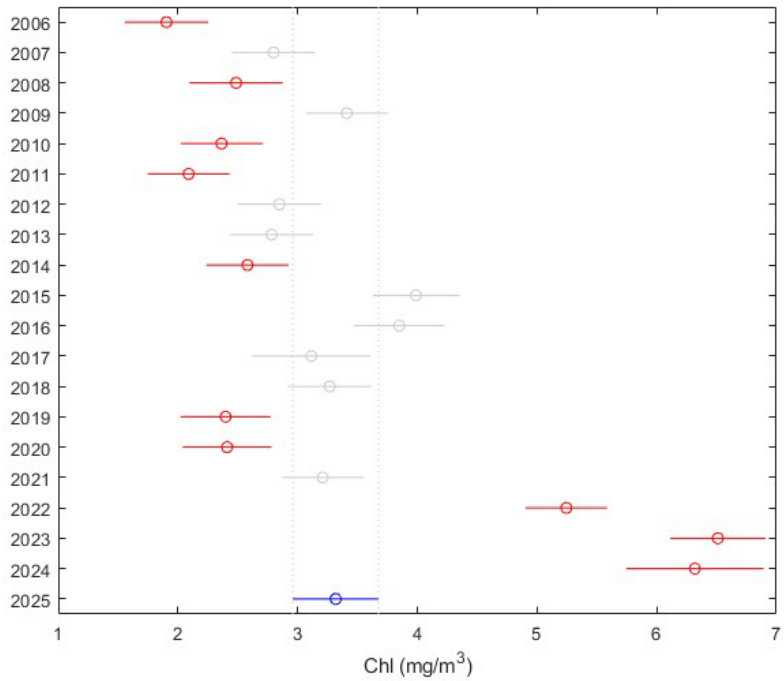

Figure 9. Comparison test of the 2025 annual median value (blue symbol) to other years. Red symbols indicate years that are significantly different, gray symbols indicate years that are statistically similar.

REFERENCES

Carberry, L., C. S. Roesler, and S. L. Drapeau. 2019. Correcting in situ chlorophyll fluorescence time series observations for non-photochemical quenching and tidal variability reveals non-conservative phytoplankton variability in coastal waters. *Limnology and Oceanography: Methods*. DOI: 10.1002/lom3.10325 https://aslopubs.onlinelibrary.wiley.com/doi/full/10.1002/lom3.10325

Proctor, C. W. and Roesler, C. S. 2010. New insights on obtaining phytoplankton concentration and composition from in situ multispectral chlorophyll fluorescence. *Limnology and Oceanography: Methods*, *8*(12): 695-708.

Roesler, C. S. 2016. In Situ Chlorophyll Fluorescence Observations on NERACOOS Mooring A01: Revised Data Flagging and Changing Phenology. Boston: *Massachusetts Water Resources Authority*. Report 2016-15. 11 p. http://www.mwra.state.ma.us/harbor/enquad/pdf/2016-15.pdf

Roesler C. S. 2020. Continuous observations of chlorophyll fluorescence and related parameters in Massachusetts Bay, 2005- 2019. Boston: *Massachusetts Water Resources Authority*. Report 2020-09. 27 p. http://www.mwra.state.ma.us/harbor/enquad/pdf/2020-09.pdf

Roesler, C. S. 2021. Continuous hourly observations of chlorophyll fluorescence, turbidity and irradiance in Massachusetts Bay 2005 – 2020. Boston: *Massachusetts Water Resources Authority*. Report 2021-11. 25 p. https://www.mwra.com/harbor/enquad/pdf/2021-11.pdf

Roesler, C. S. 2022. Continuous hourly observations of chlorophyll fluorescence, turbidity, and irradiance in Massachusetts Bay (2005 – 2021) reveal variations in phenology of phytoplankton blooms. Boston: Massachusetts Water Resources Authority. Report 2022-10. 19 p. https://www.mwra.com/media/file/2022-10pdf

Roesler, C. S. 2025. Two decades of continuous hourly observations of chlorophyll fluorescence, turbidity, and irradiance in Massachusetts Bay (2005 – 2024) reveal strengthened summertime phytoplankton blooms. Massachusetts Water Resources Authority. Report 2025-11. 20 p. https://www.mwra.com/media/file/2025-11.pdf

Roesler, C. S., J. Uitz, H. Claustre, E. Boss, X. Xing, E. Organelli, N. Briggs, A. Bricaud, C. Schmechtig, A. Poteau, F. D'Ortenzio, J. Ras, S. Drapeau, N. Haëntjens, and M. Barbieux, 2017. Recommendations for obtaining unbiased chlorophyll estimates from in situ chlorophyll fluorometers: A global analysis of WET Labs ECO sensors. *Limnology and Oceanography: Methods*, 15: 572–585. doi:10.1002/lom3.10185.

Appendix. Data file formats.

Table A1. Format of the hourly observational data file for chlorophyll fluorescence data arrays, including those derived from FLNTU and FL3-WB sensors.

Column	ID	Value/Range	Comment
1	Year	2005-2025	
2	Month	1-12	
3	Day	0-31	
4	Hour	0-25	
5	Minute	0-60	
6	Second	0-60	
7	Date.Time	732607 – 739982	MATLAB® format, decimal local standard time (EST)
8	Raw Fchl	-3.42 – 230.91	Raw hourly mean
9	Flag_Offset	0, 1	Between deployments
10	Fchl_corr_offset		Corrected for offsets
11	Flag_Biofouling1	0, 1	Biofilm
12	Flag_Biofouling2	0, 1	Structural
13	Fchl_corr_biofouling	NaN	Values removed
14	Flag_NPQ	0, 1	NPQ
15	Fchl_corr_NPQ	-1.58 - 45.19	Values corrected (Carberry et al. 2019)
16	Flag_SVO	0, 1	Single value outlier
17	Fchl_corr_SVO	NaN	Values removed
18	Flag_MDL1	0, 1	< - Method detection level (MDL)
19	Flag_MDL2	0, 1	-MDL to 0
20	Flag_MDL3	0, 1	0 to +MDL
21	Fchl_corr	-0.04 to 29.47 /NaN	Cumulative removal/correction
22	Deployment	15 – 46	Deployment number
23	ECO-FLNTU S/N	001-9999	Sensor serial number, FLNTU

Table A2. Format of the hourly observational data file for Turbidity.

Column	ID	Value/Range	Comment
1	Year	2005-2024	
2	Month	1-12	
3	Day	0-31	
4	Hour	0-25	
5	Minute	0-60	
6	Second	0-60	
7	Date.Time	732607 - 739982	MATLAB® format, decimal local standard time (EST)
8	Raw Turbidity	-0.59 to 25.95	
9	Flag_Offset	0, 1	
10	Turb_corr_offset		Corrected for offsets
11	Flag_Biofouling1	0, 1	Biofilm
12	Flag_Biofouling2	0, 1	Structural
13	Turb_corr_biofouling	NaN	Values removed
14	Flag_SVO	0, 1	Single value outlier
15	Turb_corr_SVO	NaN	Values removed
16	Flag_MDL1	0, 1	< - Method detection level (MDL)
17	Flag_MDL2	0, 1	-MDL to 0
18	Flag_MDL3	0, 1	0 to +MDL
19	Turb_corr	-0.05 to 9.81 /NaN	Cumulative removal/correction
20	Deployment	15 - 46	Deployment number
21	ECO-FLNTU S/N	001-9999	Sensor serial number, FLNTU

Table A3. Format of the hourly observational data file for downwelling irradiance (ED) and upwelling radiance (LU).

Column	ID	Value/Range	Comment
1	Year	2005-2024	
2	Month	1-12	
3	Day	0-31	
4	Hour	0-25	
5	Minute	0-60	
6	Second	0-60	
7	Date.Time	732607 - 739982	MATLAB® format, decimal local standard time (EST)
8-14	Raw Ed(7)	-33.32 - 240.31	
15	Flag_Offset	0, 1	
16-22	Ed(7)_corr_offset		Corrected for spectral and intersensor offsets
23	Flag_Biofouling	0, 1	Biofouling
24-30	Ed(7)_corr_biofouling	NaN	Values removed
31	Flag_SVO	0, 1	Single value outlier
32	Flag_MDL1	0, 1	< - Method detection level (MDL)
33	Flag_MDL2	0, 1	-MDL to 0
34	Flag_MDL3	0, 1	0 to +MDL
35	Flag Cal	0, 1	Indicates multiplicative scaling
36-42	Ed(7)_final	-0.05 – 229.45/NaN	Cumulative removal/correction
43	Deployment	15 – 46	Deployment number
44	OCI_507_SN	001-9999	OCI 507 sensor serial number

Table A4. List of submitted data arrays (.mat files) for chlorophyll fluorescence (from FLNTU sensor and each of the three channels of the F3WB sensor), turbidity, spectral irradiance, and central wavelengths of irradiance sensor.

Array Name	**Description**	**Units**	**Array size (row x columns)**	**Format**
H_Chl_49	hourly chlorophyll fluorescence, FLNTU for full time series and each deployment	mg/m3	5485x23	Table A1
H_NTU_49	hourly turbidity from FLNTU for full time series and each deployment	NTU	5485x21	Table A2
H_F1_49	Hourly chlorophyll fluorescence response from 435 nm excitation (F3WB) for full time series and each deployment	mg/m3	5485x23	Table A1
H_F2_49	Hourly chlorophyll fluorescence response from 470 nm excitation (F3WB) for full time series and each deployment	mg/m3	5485x23	Table A1
H_F3_49	Hourly chlorophyll fluorescence response from 532 nm excitation (F3WB) for full time series and each deployment	mg/m3	5485x23	Table A1
H_ED_49	Hourly spectral irradiance, 7 channels for full time series and each deployment	μW/cm2/nm	n.a.	Table A3
H_ED_49_wave	Irradiance central wavelength	nm	n.a.	n/a

Massachusetts Water Resources Authority
33 Tafts Avenue • Boston, MA 02128
www.mwra.com
617-242-6000